

Theory of the NMR relaxation rates in cuprate superconductors with field induced antiferromagnetic order

Yan Chen,¹ Jian-Xin Zhu,² and C. S. Ting¹

¹ Texas Center for Superconductivity and Department of Physics, University of Houston, Houston, TX 77204

² Theoretical Division, MS B262, Los Alamos National Laboratory, Los Alamos, NM 87545

(Dated: November 21, 2018)

Based on a model Hamiltonian with a *d*-wave pairing interaction and a competing antiferromagnetic interaction, we numerically study the site dependence of the nuclear spin resonance (NMR) relaxation rate T_1^{-1} as a function of temperature for a *d*-wave superconductor (DSC) with magnetic field induced spin density wave (SDW) order. In the presence of the induced SDW, we find that there exists no simple direct relationship between NMR signal rate T_1^{-1} and low energy local density of states while these two quantities are linearly proportional to each other in a pure DSC. In the vortex core region, T_1^{-1} on ^{17}O site may exhibit a double-peak behavior, one sharp and one broad, as the temperature is increased to the superconductivity transition temperature T_c , in contrast to a single broad peak for a pure DSC. The existence of the sharp peak corresponds to the disappearance of the induced SDW above a certain temperature T_{AF} which is assumed to be considerably lower than T_c . We also show the differences between T_1^{-1} on ^{17}O and that on ^{63}Cu as a function of lattice site at different temperatures and magnetic fields. Our results obtained from the scenario of the vortex with induced SDW is consistent with recent NMR and scanning tunneling microscopy experiments.

PACS numbers: 76.60.-k, 74.60.Ec, 74.25.Ha

I. INTRODUCTION

Intensive efforts have been focused recently on the nature of low-lying excitation spectra around a vortex core in high temperature superconductors (HTS). The excitations around the core play a fundamental role in determining physical property of a superconductor. It has now been established both experimentally^{1,2,3,4,5,6} and theoretically^{7,8,9,10,11,12,13,14,15,16} that a spin density wave (SDW) order could be induced and pinned at the vortex lattice by a strong magnetic field for both under- and optimally-doped HTS. In neutron scattering experiments by Lake *et al.*¹, a remarkable antiferromagnetic (AF)-like SDW was observed in optimally- and under-doped $\text{La}_{2-x}\text{Sr}_x\text{CuO}_4$ under a strong magnetic field. The muon spin rotation measurement by Miller *et al.*² studied the internal magnetic field distribution in the vortex core of underdoped $\text{YBa}_2\text{Cu}_3\text{O}_{6+x}$, and it was revealed a feature in the high-field tail which fits well to a model with static alternating magnetization. Recent nuclear magnetic resonance (NMR) measurements by Mitrovic *et al.*³ studied the spatially resolved NMR signal in the mixed state of optimally doped $\text{YBa}_2\text{Cu}_3\text{O}_{7-\delta}$, and they found strong AF fluctuations outside the cores and rather different electronic states inside the vortex cores. Another NMR experiment by Kakuyanagi *et al.*⁶ investigated the magnetism in and around the vortex core of nearly optimally-doped $\text{Tl}_2\text{Ba}_2\text{CuO}_{6+\delta}$, the NMR signal rate T_1^{-1} at Tl site provides a direct evidence that the AF spin correlation is significantly enhanced in the vortex core region. From theoretical point of view, various approaches^{7,8,9,10,11} suggest the existence of an induced AF order inside the core. Some recent studies^{12,13,14,15,16} also reveal that the AF order could propagate outside the

vortex cores and form a SDW.

As proposed in several articles^{17,18,19}, that the spatially imaging NMR experiment can be a powerful tool to investigate the exotic electronic structure around the vortex cores. The frequency dependence of NMR signal rate reflects the internal magnetic field distribution and the electronic and magnetic excitations in the mixed state can be probed through the temperature and site-dependence of T_1^{-1} . The spatial variation of the vortex lattice in the NMR experiments can be resolved by the distribution of internal magnetic field. In the present paper, we study the NMR theory for HTS with the effect of the magnetic field induced SDW being taken into account. Our approach is based upon an effective model Hamiltonian with a *d*-wave pairing interaction V_{DSC} between nearest neighboring sites and a competing onsite Coulomb repulsion U which may generate a competing AF order. The parameters are chosen in such a way that only *d*-wave superconductivity (DSC) prevails in the optimally doped HTS samples when the magnetic field $B=0$. Using the Bogoliubov-de Gennes (BdG) equations, The dynamic spin-spin correlation function between site *i* and site *j* can be numerically obtained. From this correlation function and the established methods²⁰, we are able to derive the NMR relaxation rates T_1^{-1} on ^{17}O and on ^{63}Cu nuclei, and from which the NMR signals as a function of temperature T and site location²² can be determined. Our calculation is performed for an optimally doped HTS sample with the chosen U so that the B induced SDW would appear only below a critical temperature T_{AF} which is considerably smaller than the superconductivity transition temperature T_c . We find that there exists no simple direct relationship between the NMR signal rate T_1^{-1} and the low energy local density

of states (LDOS) while these two quantities are linearly proportional to each other in a pure d -wave superconductor ($U = 0$). In the core region, we find that T_1^{-1} exhibits a double-peak behavior, one sharp and one broad, as the temperature is increased to T_c , in contrast to a single broad peak for a pure d -wave superconductor. It is found that the low temperature peak becomes sharper and moves to lower T when T_{AF} becomes lower. This result is consistent with the NMR experiments^{3,4,5,6}. We also show the differences between T_1^{-1} on ^{17}O and that on ^{63}Cu as a function of lattice site at different temperatures and magnetic fields. In general the NMR signal at the ^{63}Cu site is larger than that at ^{17}O site, and its magnitude can be quite enhanced at higher magnetic field. In section II we will outline our method and the numerical scheme for calculating the NMR relaxation rate. In section III, we will present our numerical results and their comparison with the experimental measurements. In addition we are also going to compare our work with other similar theoretically studies^{17,30,31}, there the articles^{17,30} only consider the case for a pure d -wave superconductor. In all these works^{17,30,31}, the NMR signals are calculated for the square lattice sites which may not rigorously related to the ^{17}O and ^{63}Cu sites as discussed in the present paper. In the last section, we will give a summary and discussion of our results.

II. FORMALISM

Let us begin with a phenomenological model in which interactions describing both DSC and SDW order parameters in a two-dimensional lattice are considered. The effective Hamiltonian can be written as:

$$H = - \sum_{i,j,\sigma} t_{ij} c_{i\sigma}^\dagger c_{j\sigma} + \sum_{i,\sigma} (U n_{i\bar{\sigma}} - \mu) c_{i\sigma}^\dagger c_{i\sigma} + \sum_{i,j} (\Delta_{ij} c_{i\uparrow}^\dagger c_{j\downarrow}^\dagger + h.c.) , \quad (2.1)$$

where $c_{i\sigma}^\dagger$ is the electron creation operator, μ is the chemical potential, and the summation is over the nearest neighboring sites. In the presence of magnetic field B normal to the two dimensional plane, the hopping integral can be expressed as $t_{ij} = t_0 \exp[i \frac{\pi}{\Phi_0} \int_{\mathbf{r}_i}^{\mathbf{r}_j} \mathbf{A}(\mathbf{r}) \cdot d\mathbf{r}]$ for the nearest neighboring sites (i, j) , with $\Phi_0 = h/2e$ as the superconducting flux quantum. We assume that the strength of B is large enough such that it can be regarded as uniform. Here we choose the Landau gauge for the vector potential $\mathbf{A} = (-By, 0, 0)$. Since the internal magnetic field induced by the supercurrent around the vortex core, as it will be numerically shown later, is so small as compared with B , the above assumption should be justified. The induced SDW and the DSC orders in our system are respectively defined as $\Delta_i^{SDW} = U \langle c_{i\uparrow}^\dagger c_{i\uparrow} - c_{i\downarrow}^\dagger c_{i\downarrow} \rangle$ and $\Delta_{ij} = V_{DSC} \langle c_{i\uparrow} c_{j\downarrow} - c_{i\downarrow} c_{j\uparrow} \rangle / 2$, where U and V_{DSC} represent the interaction strengths for SDW and DSC.

The mean-field Hamiltonian (1) can be diagonalized by solving the resulting BdG equations self-consistently

$$\sum_j \begin{pmatrix} \mathcal{H}_{ij,\sigma} & \Delta_{ij} \\ \Delta_{ij}^* & -\mathcal{H}_{ij,\bar{\sigma}}^* \end{pmatrix} \begin{pmatrix} u_{j,\sigma}^n \\ v_{j,\bar{\sigma}}^n \end{pmatrix} = E_n \begin{pmatrix} u_{i,\sigma}^n \\ v_{i,\bar{\sigma}}^n \end{pmatrix} , \quad (2.2)$$

where the single particle Hamiltonian $\mathcal{H}_{ij,\sigma} = -t_{ij} + (U n_{i\bar{\sigma}} - \mu) \delta_{ij}$, and $n_{i\uparrow} = \sum_n |u_{i\uparrow}^n|^2 f(E_n)$, $n_{i\downarrow} = \sum_n |v_{i\downarrow}^n|^2 (1 - f(E_n))$, $\Delta_{ij} = \frac{V_{DSC}}{4} \sum_n (u_{i\uparrow}^n v_{j\downarrow}^{n*} + v_{i\downarrow}^n u_{j\uparrow}^n) \tanh\left(\frac{E_n}{2k_B T}\right)$, with $f(E)$ as the Fermi distribution function and the electron density $n_i = n_{i\uparrow} + n_{i\downarrow}$. The DSC order parameter at the i th site is $\Delta_i^D = (\Delta_{i+e_x,i}^D + \Delta_{i-e_x,i}^D - \Delta_{i+e_y,i}^D - \Delta_{i-e_y,i}^D)/4$ where $\Delta_{ij}^D = \Delta_{ij} \exp[i \frac{\pi}{\Phi_0} \int_{\mathbf{r}_i}^{\mathbf{r}_j} \mathbf{A}(\mathbf{r}) \cdot d\mathbf{r}]$ and $\mathbf{e}_{x,y}$ denotes the unit vector along (x, y) direction. The main procedure of our self-consistent calculation is summarized as follows. For a random set of initial parameters $n_{i\sigma}$ and Δ_{ij} , the Hamiltonian is numerically diagonalized and the obtained quasiparticle wave functions $u_{i,\sigma}^n$ and $v_{i,\sigma}^n$ are used to calculate the new parameters for the next iteration step. The iteration continues until the relative difference of order parameter between two consecutive iteration steps is less than 10^{-4} .

In the following section, we need to calculate the local density of states (LDOS) according to the formula:

$$\rho_i(E) = - \sum_n [|u_{i\uparrow}^n|^2 f'(E_n - E) + |v_{i\downarrow}^n|^2 f'(E_n + E)] , \quad (2.3)$$

where $f'(E) \equiv df(E)/dE$. The LDOS is proportional to the local differential tunneling conductance at low temperature which can be measured by STM experiments. In addition, we also need to calculate the internal magnetic field distribution of the vortex state. The internal magnetic field is computed through the Maxwell equation, $\nabla \times \mathbf{H}_{int}(\mathbf{r}) = \frac{4\pi}{c} \mathbf{j}(\mathbf{r})$, where the current $\mathbf{j}(\mathbf{r})$ is calculated as:

$$j_{\mathbf{e}_{x,y}}(\mathbf{r}_i) = 2|e| \text{Im} \{ t_{i+\mathbf{e}_{x,y},i} \sum_n [u_{i+\mathbf{e}_{x,y}}^{n*} u_i^n f(E_n) + v_{i+\mathbf{e}_{x,y}}^n v_i^{n*} (1 - f(E_n))] \} . \quad (2.4)$$

The nuclear spin relaxation rate T_1^{-1} can be obtained from the spin-spin correlation function $\chi_{+,-}(i, j, \Omega)$ at zero energy through the following site dependent function^{17,25},

$$\begin{aligned} R(i, j) &= \text{Im} \chi_{+,-}(i, j, i\Omega_n \rightarrow \Omega + i\eta) / (\Omega/T)|_{\Omega \rightarrow 0} \\ &= - \sum_{n,n'} u_i^n u_{j'}^{n'*} [u_j^n u_{j'}^{n'*} + v_j^n v_{j'}^{n'*}] \\ &\quad \times \pi T f'(E_n) \delta(E_n - E_{n'}). \end{aligned} \quad (2.5)$$

Since all of the experiments^{3,4,5,6} are performed at the oxygen, copper, or other nuclei in HTS, we need the expressions of the NMR relaxation rate at these sites. In this paper we shall mainly consider the contribution from the planar oxygen (^{17}O) and copper (^{63}Cu) nuclei. The

oxygen nucleus is located between two *Cu* nuclei along the *x* or *y* axis. The internal magnetic field H_{int} on ^{17}O site is averaged over its two nearest neighboring ^{63}Cu sites. The NMR relaxation rate form factor on nuclei ^{17}O and ^{63}Cu in momentum space is: $F_{O,x} \sim 1 + \cos(q_x/2)$ and $F_{Cu} \sim (\cos(q_x) + \cos(q_y))^2$. It can be expressed in terms of the real-space spin-spin correlations as follows²⁰:

$$1/^{17}T_1T = C[R(i,i) + 1/2 \sum_{j,x} R(i,j)], \quad (2.6)$$

$$1/^{63}T_1T = B[R(i,i) + 1/2 \sum_j R(i,j) + 1/4 \sum_j R(i,j)], \quad (2.7)$$

here the notation of \sum'_x , \sum''_x and \sum'''_x means summation over two nearest-neighboring sites along the *x* axis, four next-neighboring-sites, and four next-next-neighboring sites, respectively. Here we calculate T_1^{-1} in terms of arbitrary unit and choose the ratio of the coefficients²¹ $B/C = 1.583$.

Throughout this paper, we use the following parameters: $U = 2.4$, $V_{DSC} = 1.2$, the linear dimension of the unit cell of the vortex lattice is chosen as $N_x \times N_y = 40 \times 20$ sites and the number of the unit cells $M_x \times M_y = 20 \times 40$, and the hole doping level $x = 0.15$. This choice corresponds to a uniform magnetic field $B \simeq 37T$. We set $t_0 = a = 1$. The standard procedures²⁶ are followed to introduce magnetic unit cells, where each unit cell contains two superconducting flux quanta. By introducing the quasi-momentum of the magnetic Bloch state, we obtain the wave function under the periodic boundary condition whose region covers many unit cells.

III. NUMERICAL RESULTS AND COMPARING WITH EXPERIMENTS

Our previous numerical calculations¹² show clearly that the induced AF order exists both inside and outside the vortex cores, and behaves like an inhomogeneous SDW with the same wave length in the *x* and *y* directions. Fig. 1 depicts the SDW amplitude or the staggered magnetization $M_i^s = \Delta_i^{SDW}/U$ distribution in a square lattice. It is seen that the induced SDW order reaches its maximum value at the vortex core center (V), zero value at the saddle-point midway between two nearest neighboring vortices (S), and in between at the center of the squared vortex lattice unit cell (C). Using Eq.(2.4), the internal magnetic field H_{int} at different site can be numerically determined. In the upper right inset of Fig. 1 we show the histogram of H_{int} , where $P(H_{int})$ measures the number of lattice sites (or plaquettes) with fixed H_{int} . We can approximately identify each site (V, S, C) including the sites around it in the vortex lattice

to the distribution. The correspondence between the site position and H_{int} can roughly be established. It is easy to see that the magnitude of H_{int} is decreasing along the path (V→S→C) and its direction is always perpendicular to the lattice plane. In a narrow region, H_{int} may even become negative. This is very different from the case for a pure DSC where H_{int} is always positive¹⁷. Our histogram of H_{int} distribution is consistent with the experimental data³ except there the region of negative H_{int} is somewhat wider than ours. The experimentally observed negative H_{int} may indicate the existence of magnetic field induced SDW around the vortex cores.

The NMR signal at the maximum cutoff of the histogram as a function of internal magnetic field comes from the V-site. The minimum cutoff is from the C-site. The peak value of the internal magnetic field comes from the S-site. Contrary to the case for a pure *d*-wave superconductor, the SDW order outside the vortex core may have a remarkable contribution to both the internal magnetic distribution and the NMR signal. It is supposed that ^{17}O NMR experiment can provide direct information on the LDOS as the antiferromagnetism spin fluctuation is cancelled^{27,28}. From our study, we find that in the presence of SDW vortex cores, the internal magnetic field on ^{17}O site can not be cancelled exactly and appreciable residue exists.

Next, we study the relationship between low energy

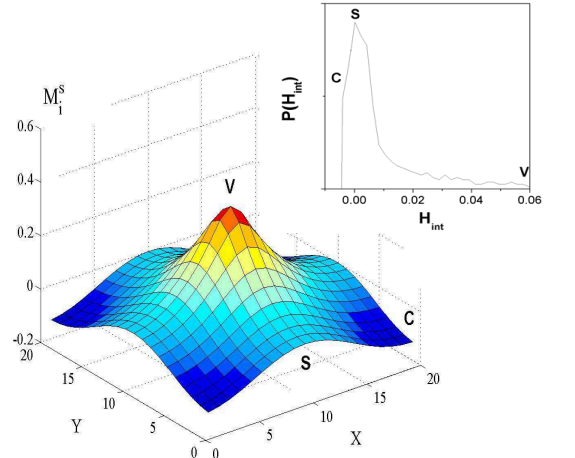


FIG. 1: The amplitude distribution of the SDW order parameter M_i^s (a) in one magnetic unit cell. V, S, C points represents the vortex core center, the saddle point midway between two nearest neighboring vortices, and the center of the squared vortex lattice unit cell, respectively. The inset shows the histogram $P(H_{int})$ of the induced magnetic field distribution where H_{int} is in a unit of 10^3 Gauss. The calculation is performed with $U = 2.4$ and $V_{DSC} = 1.2$.

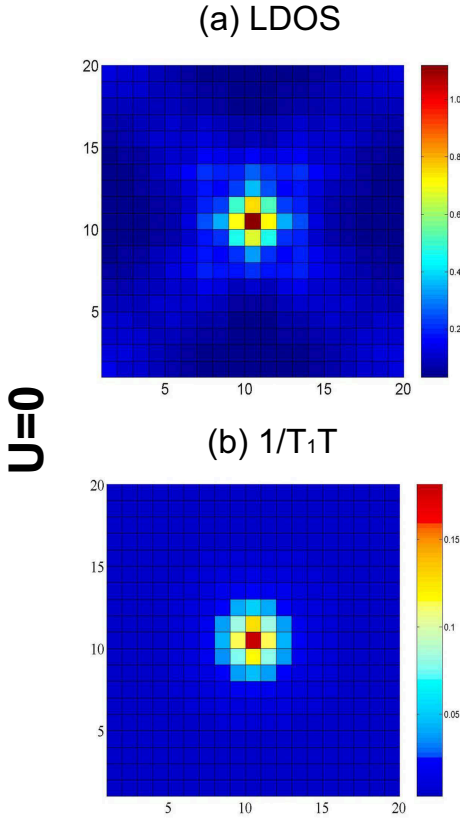


FIG. 2: The spatial distribution images of the LDOS at the energy $E = 0$ (a) and NMR relaxation rate $1/T_1(i)T$ (b) in a vortex unit cell for a pure DSC with $U=0$. Other parameter values are the same as those in Fig. 1.

LDOS and NMR signal rate $1/T_1$. In a pure d -wave superconductor(DSC), a linear relationship is found between $1/T_1(i) \sim R(i, i)$ and the LDOS $\rho_i(E = 0)^{17}$ at zero temperature. We have checked our program and reproduced similar results. Figure 2 depicts the spatial distribution images of LDOS $\rho_i(E = 0)$ (a), and $1/T_1(i)T$ (b) for a pure DSC with $U=0$ at low temperature. In this case, the core state shows zero-energy peak²⁶ and nodal directions are along $x = y$ and $x = -y$. The images in Fig. 2(a) and 2(b) are similar to each other and the results can be regarded as linearly proportional to each other. Thus the NMR signal for a pure DSC can be estimated quantitatively from its corresponding zero energy LDOS according to the linear relationship.

From Fig. 2(a), the LDOS of quasiparticles decreases along the path (V \rightarrow C \rightarrow S). In the nodal directions, appreciable weight of the low-energy states extending from the vortex core still remains there. Our numerical result indicates that the LDOS of the low-energy states at the C-site is slightly larger than that of the S-site, although C-site is farther away from the vortex center. This is different from the work by Takigawa *et al.*¹⁷ where the LDOS at the S site is found to be larger than that

at the C site. The authors¹⁷ there employed the symmetrical gauge and they found that their unit vector of vortex lattice is oriented along 45° from the Cu-O bond. But our result is consistent with the study of Knapp *et al.*³⁰ who used a different approach and calculated the NMR signal at various sites for a pure DSC. Furthermore, a recent small-angle neutron scattering measurement²⁹ for $\text{La}_{1.83}\text{Sr}_{0.17}\text{CuO}_{4+\delta}$ indicates that the unit vector of vortex lattice is clearly oriented along the Cu-O bonds, consistent with our result in Fig. 1. The NMR experiments^{3,4,5,6} also show that the NMR signal first decreases as one moves away from the V-site to S-site and then increases at the C-site, consistent with the results in Fig. 2. Here we notice that the NMR signal at C site is slightly larger than that at S-site, their difference could be seen in Fig. 6 and Fig. 7. It appears that the above analysis could provide a basic understanding of the spatial distribution of the experimentally observed NMR relaxation rates in HTS in the framework of pure DSC. However, it is well known that the theoretical predicted LDOS²⁶, which shows a strong zero energy peak for a pure DSC at the vortex core is in contradictory to the STM measurements^{23,24} on HTS. In order to overcome this difficulty, the magnetic induced AF order has been introduced¹¹ to account for the experiments. In the following we shall investigate the effect of induced AF or SDW order on the NMR theory in HTS.

The presence of the induced SDW order in the mixed state may lead to violation of the linear relationship between the LDOS at $E=0$ and the NMR relaxation rate $1/T_1(i)$. This can be seen clearly in Fig. 3, where we show the spatial images of the LDOS (a) and the $1/T_1(i)T$ (b) according to our numerical calculations for $U=2.4$. There is little resemblance between Figs. 3(a) and 3(b), and the linear relationship does not exists here. Fig. 3(a) indicates that the LDOS is smallest at V-site, and largest at S-site, it clearly can not be applied to explain the NMR experiments^{3,4,5,6} as in the case for a pure DSC. But the LDOS obtained here exhibits no zero energy peak at the vortex core which is consistent with the STM experiments^{23,24}. The averaged LDOS of quasiparticles in Fig. 3(a) ($U=2.4$) is greatly suppressed than that in Fig. 2(a) ($U=0$). This is because the presence of the induced SDW enhances the insulating nature of the system and thus reduces the number of the quasiparticles. When $U=2.4$, there are two contributions to the NMR signal $1/T_1(i)T$, at the low temperature, the dominant one is from the induced SDW order and the minor one is from the low energy quasiparticle states. The LDOS is the smallest at the vortex core center but the SDW order is at its maximum as shown in Fig. 1. From Fig. 3(b), it is easy to see that the spatially distributed NMR signal $1/T_1(i)T$ which has the largest value at the vortex center because of the induced AF order there and decreases along the path (V \rightarrow C \rightarrow S). This feature is consistent with what has been observed by the experiments^{3,4,5,6} and in sharp contrast with Takigawa *et al.*'s results³¹. They claimed that T_1^{-1} at V-site is smaller than the neigh-

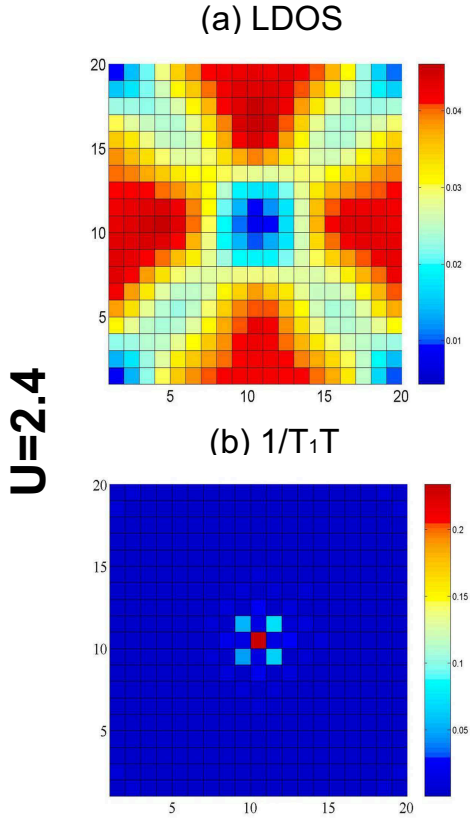


FIG. 3: The spatial distribution images of the LDOS at the energy $E = 0$ (a) and NMR relaxation rate $1/T_1(i)T$ (b) in a vortex unit cell for a DSC with induced SDW. All parameter values are the same as those in Fig. 1.

boring sites and the NMR signal rate at S-site is higher than that of C-site. The choice of lattice size in their calculations corresponds to a very strong magnetic field at about 51 Tesla. Their results seem to be inconsistent with the measurement of $1/^{17}T_1$ on $\text{YBa}_2\text{Cu}_3\text{O}_{7-\delta}$ ³.

The NMR signals also exhibit the temperature T and magnetic field B dependences. Our approach described in Section II is easily extended to study the finite T case, but not the B dependence because weaker B implies larger size calculation which we are not able to do at the present moment. Since the observed NMR signals are coming from the oxygen, copper, or other atoms in HTS, here we shall mainly consider the temperature dependence of the NMR signal rate $1/^{17}T_1$ from the ^{17}O sites using Eq. (2.6). It needs to be point out that the value of $R(i, j \neq i)$ in Eq. (2.6) is of the same order with $R(i, i)$ and its contribution should not be neglected. In Fig. 4, the NMR relaxation rates $1/T_1=1/^{17}T_1$ on ^{17}O site normalized by its value $1/T_1^c$ at T_c as a function of T are plotted for sites V, C and S. The calculations are performed using $U=2.4$ except the dashed curve associated with the V site where $U=0$ and is obtained for a pure DSC. The inset plots the temperature dependence

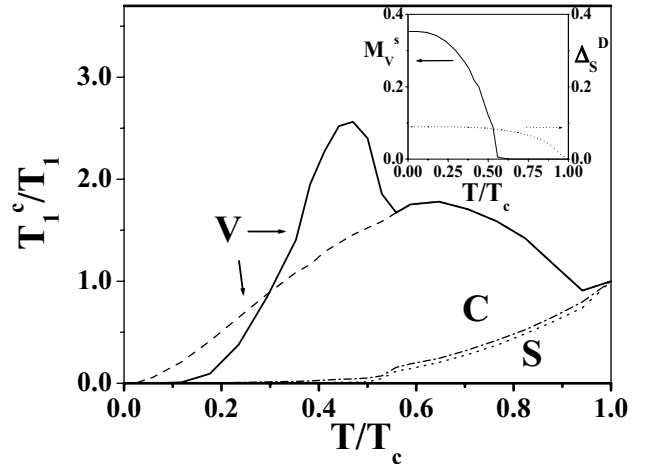


FIG. 4: Temperature dependences of ^{17}O NMR signals $1/T_1$ normalized by its value $1/T_1^c$ at T_c are plotted as a function of T/T_c at the sites V, S, C. The dashed line associated with the site V is obtained for a pure DSC by using $U=0$. The inset plots the temperature dependence of SDW order parameters at V-site and DSC order at S-site.

of the staggered magnetization at V-site and DSC order at S-site. Our calculations show that the vast majority sites outside the vortex core exhibit long relaxation time, but few sites around the vortex core exhibit short relaxation time, which contains useful information on the site-dependent low energy excitations around the vortex. The maximum magnitude of $^{17}T_1^{-1}$ at V-site is about two orders of magnitude larger than that far from the vortex core, and the NMR signal rate at C-site is also larger than that at S-site. Because both NMR signals at C and S sites are very weak as compared to that at V site, their distinction is not reflected in Fig. 4 below $T < 0.4T_c$. The minimal value of the staggered magnetization occurs near the saddle point S. It reflects the fact that the SDW order at C site is larger than that at S site as shown in Fig. 1. This result clearly indicates that the presence of the induced SDW order makes remarkable contribution to NMR signals. At the vortex core center V, the evolution of T_1^{-1} with temperature exhibits a double peak structure below T_c ; the sharp peak occurs at lower T and the broad peak is at higher T . This is in contrast to a single peak obtained with $U=0$ for a pure DSC¹⁷, and it can be clearly seen from the dashed curve below a critical temperature $T_{AF} \sim 0.54T_c$ and the solid curve above T_{AF} associated with the V site in Fig. 4. The inset shows that above the temperature T_{AF} , the induced staggered magnetization vanishes and only DSC order prevails up to T_c . The sharp peak at $0.45T_c$ is below T_{AF} and the broad peak at $0.64T_c$ is originated in the pure DSC order. It is obvious that the value of the critical temperature T_{AF} is U or sample dependent, and the position of the sharp peak can be made to a lower T if a smaller U or T_{AF} is chosen for the calculation. In

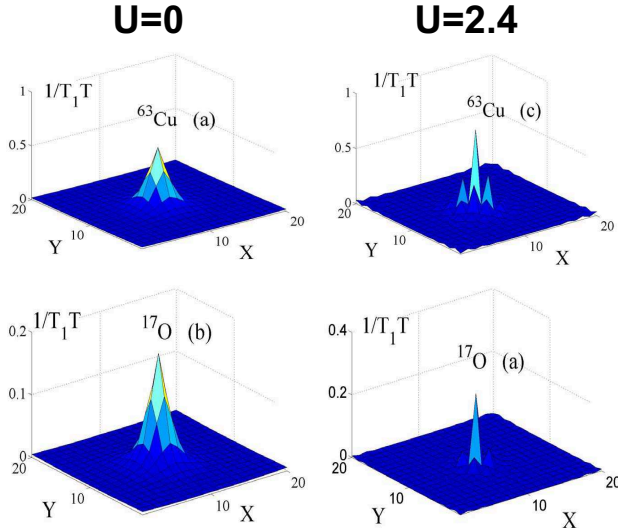


FIG. 5: Site-dependent relaxation rate T_1^{-1} for ^{63}Cu (a), ^{17}O nuclei of pure d -wave case and ^{63}Cu (c), ^{17}O (d) site of SDW vortex core case.

case the value of T_{AF} is slightly higher than the position of the broad peak, only a single peak for the NMR signal is predicted. When T_{AF} is close or larger than T_c , the NMR signal would be a increasing function of T and may not show any peak structure. We also have done the same calculation for the NMR relaxation rates on ^{63}Cu nuclei on our model lattice sites ($1/T_1(i)$), and found similar T and site dependence as shown in Fig. 4. In the experimental aspect, a sharp peak has been observed at $T \sim 0.235T_c$ ⁶ in $\text{Tl}_2\text{Ba}_2\text{CuO}_6$ while there is no observed peak in $\text{YBa}_2\text{Cu}_3\text{O}_7$ up to $T \sim 0.272T_c$ ³. Therefore the value U in $\text{YBa}_2\text{Cu}_3\text{O}_7$ should be larger than that in $\text{Tl}_2\text{Ba}_2\text{CuO}_6$. This conclusion is opposite to the theoretical prediction made by Takigawa *et al.*³¹

We also would like to examine the difference in the spatial distributions of the NMR signals from ^{63}Cu and ^{17}O nuclei. In Fig. 5, The site distribution maps of T_1^{-1} for ^{63}Cu and for ^{17}O in a pure DSC ($U=0$) are respectively illustrated in (a) and (b). Both of these maps reach a similar peak value at the vortex core and then fall away smoothly from it. In the vortex core, the magnitude of T_1^{-1} at the ^{63}Cu site is about three times larger than that at the ^{17}O site. In Figs. 5(c) and 5(d), we present the results for ^{63}Cu and ^{17}O nuclei in a DSC with induced SDW ($U=2.4$). The site-dependent spectra for both nuclei show staggered oscillations in the vortex core, there the NMR signal rate from the ^{17}O site is about one fourth of the value from that of ^{63}Cu site. This is because the AF order at the ^{17}O sites could be dramatically weakened by the partial cancellation of the staggered magnetization between two nearest neighboring sites on the original lattice. It is useful to point out that the NMR signal $^{17}T_1^{-1}$ outside the vortex core region is one order of magnitude smaller than that of $^{63}T_1^{-1}$. In the presence

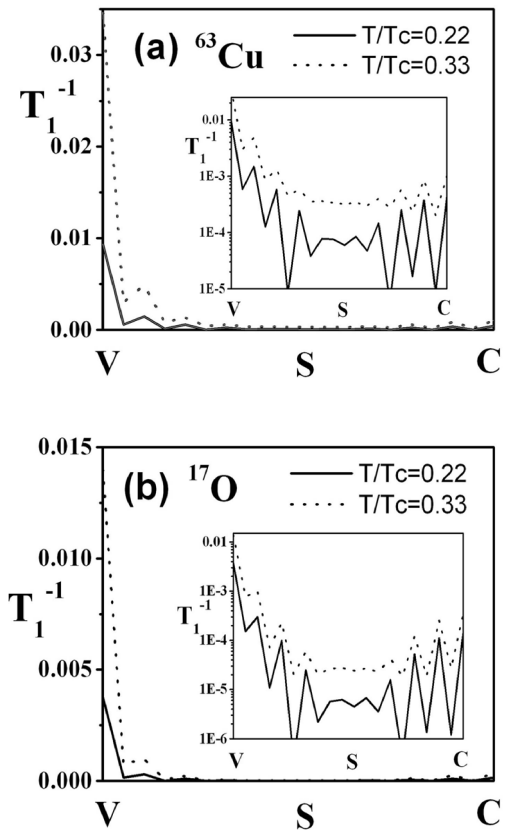


FIG. 6: Site-dependent relaxation rate T_1^{-1} for two different temperatures with $U=2.4$ and the magnetic field $B=37\text{T}$ at ^{63}Cu (a) and at ^{17}O (b). The log plot is shown as inset.

of the induced SDW, the NMR signal rate is enhanced at the core center and suppressed away from the vortex core. For both $U=0$ and $U=2.4$ cases, T_1^{-1} reaches a maximum at the core center while its value at the C-site is always larger than that at the S-site.

Next, the temperature dependence of NMR signal rates for the case of $U=2.4$ is examined. Here, we plot the variation of T_1^{-1} along the path $V \rightarrow S \rightarrow C$ for ^{63}Cu nuclei in Fig. 6(a) and for ^{17}O nuclei Fig. 6(b) at two different temperatures. The values of T_1^{-1} in Figs. 6(a) and 6(b) exhibit similar behavior and oscillate from site to site. The amplitude of the oscillation reflects the underlying staggered magnetization and is apparently weakened at higher temperature. In fact, the T dependence of NMR signal rate at three typical points has been seen from Fig. 3. Figure 6 shows more clearly that NMR signal rate at each site increases with temperature and its value at site C is always larger than that at site S. We have reproduced the power law relation $T_1^{-1} \sim T^3$ for a pure DSC¹⁷ at zero magnetic field and at low temperature.

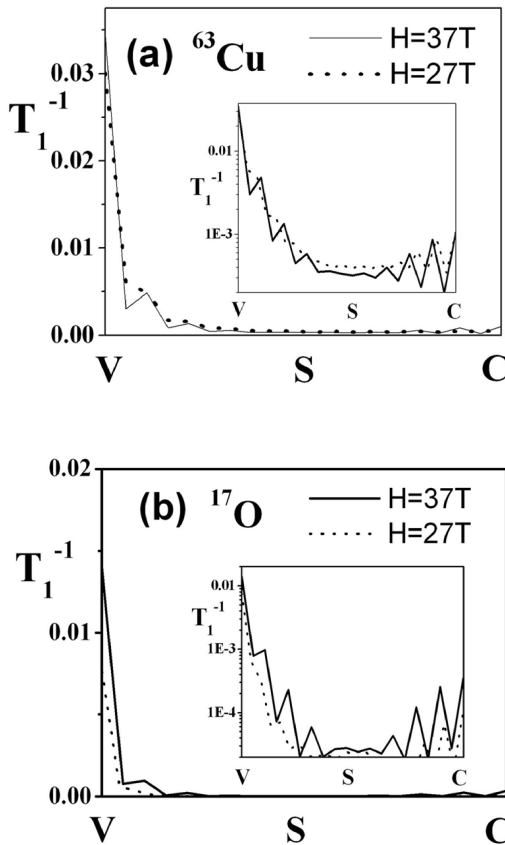


FIG. 7: Site-dependent relaxation time T_1^{-1} for two different magnetic fields with $U=2.4$ and the temperature $T/T_c=0.35$ at ^{63}Cu (a) and at ^{17}O (b). The log plot is shown as inset.

In the presence of vortices with induced SDW order, it should not be surprised that T_1^{-1} does not follow this T^3 law.

Finally, we show the site dependence of NMR signal rates on ^{63}Cu and on ^{17}O nuclei at two different magnetic field B respectively in Figs. 7(a) and 7(b). The NMR signals T_1^{-1} in Figs. 7(a) and 7(b) are similar to each other. Since the magnitude of the induced SDW order is strongly dependent on the external magnetic field B — higher B leads to more pronounced SDW order which may in turn yield a larger NMR signal. This conclusion is consistent with the NMR experiments⁶. As a result, the amplitude of oscillation at different sites, which measures the strength of the induced staggered magnetization, is dramatically reduced when the magnetic field B is decreased from 37T to 27T as shown in Fig. 7. Here $B = 27\text{T}$ corresponds to a vortex lattice unit cell of 48×24 sites. On the other hand, the NMR signal rate at V-site is suppressed with increasing B for a pure DSC¹⁷ which reflects the density of quasiparticle

around the vortex core is reduced due to the enhancement of quasiparticle leakage along the nodal directions. It was argued by Takigawa et al.³¹ that when AF order inside the vortex core is large enough, T_1^{-1} becomes the absolute minimum at V-site. This conjecture³¹ is based on the assumption that the linear relation between T_1^{-1} and LDOS still exists even in the presence of the SDW order. On the other hand, our results indicate strongly that with the increasing B , the enhancement of AF order inside the vortex core may lead to more pronounced T_1^{-1} value at the V-site. This is very different from what has been predicted in Ref. 31. Finally we point out that existing experimental data³ show the presence of appreciable NMR signal rate at S-site and its value is insensitive to T . But in our calculations there is a very weak NMR signal at S-site. The discrepancy between experimental data and our results may be due to the reason unclear to us at this moment.

IV. SUMMARY

Based on a model Hamiltonian as described in Sections I and II, we have investigated the site- and temperature-dependence of NMR signal rate T_1^{-1} near the vortex core in an optimally doped HTS. The calculations are carried out with ($U = 2.4$) and without ($U = 0$) the magnetic field induced SDW order. Although the relative values of T_1^{-1} at V, S, and C sites near the vortex core obtained theoretically for a pure DSC are consistent with recent experiments^{3,4,5,6}, the temperature dependent of T_1^{-1} thus derived fails to explain the sharp peak observed in NMR experiments⁶ for $\text{Ti}_2\text{Ba}_2\text{CuO}_{6+\delta}$ at low temperature. Moreover, the LDOS obtained for a pure DSC²⁶ has a zero energy peak at the core center and this is in contradictory to the STM observations^{23,24}. All these difficulties could somewhat be removed by introducing the field induced SDW pinned at the vortex cores as it has been studied in the present paper. With the induced SDW order, the LDOS exhibits no zero energy peak at the core center and is consistent with experiments. Unlike the case for a pure DSC, there exists no linear relationship between zero energy LDOS and T_1^{-1} . We show that SDW order could strongly enhance the NMR signal rate, and as a result, the NMR signal T_1^{-1} from ^{17}O site has its largest value at the core center V, and smallest value at the saddle point S site (see Figs. 6 and 7). The temperature dependent of T_1^{-1} at V site exhibits a sharp peak at low temperature which is in agreement with the NMR experiments^{3,6}. Since the strength of the SDW order depends on the magnitude of B , the value of T_1^{-1} should also be enhanced by increasing B . We also compare T_1^{-1} from ^{63}Cu and ^{17}O nuclei at different T and B , their essential features are similar to each other. The magnitude of $^{17}T_1^{-1}$ outside the vortex core region is about one order of magnitude smaller than that of $^{63}T_1^{-1}$ while these two values are closer to each other inside the vortex core. Finally, we would like to point out that

the difference between our results and those of a similar work³¹ has been discussed in detail in Section III. Another fundamental difference is that their LDOS³¹ at the vortex center for a pure DSC ($U = 0$) shows double peaks near $E=0$ while only a single peak is obtained in previous²⁶ and present works. It is our hope that the present calculation may shed more light on the understanding of recent NMR and STM experiments for the mixed state of HTS in a unified picture, and stimulate more theoretical activity in this field.

Acknowledgments

We are grateful to S. H. Pan, B. Friedman, G. -q. Zheng and Z. D. Wang for useful discussions. This work was supported by a grant from the Robert A. Welch Foundation and by the Texas Center for Superconductivity at the University of Houston through the State of Texas (YC and CST), and the Department of Energy (JXZ).

¹ B. Lake, G. Aeppli, K.N. Clausen, D.F. McMorrow, K. Lefmann, N.E. Hussey, N. Mangkorntong, M. Nohara, H. Takagi, T.E. Mason, and A. Schröder, *Science* **291**, 1759 (2001); B. Lake, H.M. Ronnow, N.B. Christensen, G. Aeppli, K. Lefmann, D.F. McMorrow, P. Vorderwisch, P. Smeibidl, N. Mangkorntong, T. Sasagawa, M. Nohara, H. Takagi, and T.E. Mason, *Nature* **415**, 299 (2002).

² R.I. Miller, R.F. Kiefl, J.H. Brewer, J.E. Sonier, J. Chakhalian, S. Dunsiger, G.D. Morris, A.N. Price, D.A. Bonn, W.H. Hardy, and R. Liang, *Phys. Rev. Lett.* **88**, 137002 (2002).

³ V.F. Mitrovic, E.E. Sigmund, M. Eschrig, H.N. Bachman, W.P. Halperin, A.P. Reyes, P. Kuhns, and W.G. Moulton, *Nature* **413**, 501 (2001); V.F. Mitrovic, E.E. Sigmund, W.P. Halperin, A.P. Reyes, P. Kuhns, and W.G. Moulton, cond-mat/0202368 (unpublished).

⁴ N.J. Curro, C. Milling, J. Hasse, and C.P. Slichter, *Phys. Rev. B* **62**, 3473 (2000).

⁵ K. Kakuyanagi, K. Kumagai, and Y. Matsuda, *Phys. Rev. B* **65**, 060503 (2002).

⁶ K. Kakuyanagi, K. Kumagai, Y. Matsuda, and M. Hasegawa, cond-mat/0206362 (unpublished).

⁷ S.-C. Zhang, *Science* **275**, 1089 (1997); D.P. Arovas, A. J. Berlinsky, C. Kallin, and Shou-Cheng Zhang, *Phys. Rev. Lett.* **79**, 2871 (1997).

⁸ E. Demler, S. Sachdev, and Y. Zhang, *Phys. Rev. Lett.* **87**, 067202 (2001); Y. Zhang, E. Demler, and S. Sachdev, *Phys. Rev. B* **66**, 094501 (2002).

⁹ M. Ogata, *Int. J. Mod. Phys. B* **13**, 3560 (1999).

¹⁰ M. Ichioka, M. Takigawa and K. Machida, *J. Phys. Soc. Jpn.* **70**, 33 (2001).

¹¹ Jian-Xin Zhu and C.S. Ting, *Phys. Rev. Lett.* **87**, 147002 (2001).

¹² Yan Chen and C.S. Ting, *Phys. Rev. B* **65**, R180513 (2002).

¹³ Jian-Xin Zhu, Ivar Martin, and A.R. Bishop, *Phys. Rev. Lett.* **89**, 067003 (2002).

¹⁴ Yan Chen, H.Y. Chen and C.S. Ting, *Phys. Rev. B* **66**, 104501 (2002).

¹⁵ Han-Dong Chen, Jiang-Ping Hu, Sylvain Capponi, Enrico Arrigoni, and Shou-Cheng Zhang, *Phys. Rev. Lett.* **89**, 137004 (2002).

¹⁶ M. Franz, D.E. Sheehy, and Z. Tesanovic, *Phys. Rev. Lett.* **88**, 257005 (2002).

¹⁷ M. Takigawa, M. Ichioka, and K. Machida, *Phys. Rev. Lett.* **83**, 3057 (1999); *J. Phys Soc. Jpn.* **69**, 3943 (2000).

¹⁸ R.Wortis, A.J. Berlinsky, and C. Kallin, *Phys. Rev. B* **61**, 12342 (2000).

¹⁹ D.K. Morr and R. Wortis, *Phys. Rev. B* **61**, R882 (2000), and D.K. Morr, *Phys. Rev. B* **63**, 214509 (2001).

²⁰ B.S. Shastry, *Phys. Rev. Lett.* **63**, 1288 (1989); A.J. Millis, H. Monien, and D. Pines, *Phys. Rev. B* **42**, 167 (1990); Z.Y. Weng, D.N. Sheng, and C.S. Ting, *Phys. Rev. B* **59**, 11367 (1999).

²¹ N. Bulut, D. Hone, D.J. Scalapino, and N.E. Bickers, *Phys. Rev. Lett.* **64**, 2723-2726 (1990).

²² Some preliminary results have been reported in, C.S. Ting, Yan Chen, and Jian-Xin Zhu, *Bull. Am. Phys. Soc.* **47** (1), 330 (2002) [March].

²³ Ch. Renner, B. Revaz, K. Kadowaki, I. Maggio-Aprile, Ø. Fischer, *Phys. Rev. Lett.* **80**, 3606 (1998).

²⁴ S.H. Pan, E.W. Hudson, A.K. Gupta, K.-W. Ng, H. Eisaki, S. Uchida, and J.C. Davis, *Phys. Rev. Lett.* **85**, 1536 (2000).

²⁵ R. Leadon, and H. Suhl, *Phys. Rev.* **165**, 596 (1968).

²⁶ Y. Wang and A.H. MacDonald, *Phys. Rev. B* **52**, R3876 (1995).

²⁷ M. Takigawa, A.P. Reyes, P.C. Hammel, J.D. Thompson, R.H. Heffner, Z. Fisk, and K.C. Ott, *Phys. Rev. B* **43**, 247 (1991).

²⁸ N. Bulut and D.J. Scalapino, *Phys. Rev. B* **45**, 2371 (1992).

²⁹ R. Gilardi, J. Mesot, A. Drew, U. Divakar, S.L. Lee, E.M. Forgan, O. Zaharko, K. Conder, V.K. Aswal, C.D. Dewhurst, R. Cubitt, N. Momono, and M. Oda, *Phys. Rev. Lett.* **88**, 217003 (2002).

³⁰ D. Knapp, C. Kallin, A.J. Berlinsky, and R. Wortis, *Phys. Rev. B* **66**, 144508 (2002).

³¹ M. Takigawa, M. Ichioka, and K. Machida, *Phys. Rev. Lett.* **90**, 047001 (2003).